Phonon-induced quantum diffusion in Carbon-based materials

2015 J. Phys.: Conf. Ser. 647 012045

(http://iopscience.iop.org/1742-6596/647/1/012045)

Journal of Physics: Conference Series **647** (2015) 012045 doi:10.1088/1742-6596/647/1/012045

Phonon-induced quantum diffusion in Carbon-based materials

R Rosati[1], F Dolcini[1,2] and F Rossi[1]

1 Department of Applied Science and Technology, Politecnico di Torino, C.so Duca degli Abruzzi 24, 10129 Torino, Italy
2 CNR-SPIN, Monte S.Angelo - via Cinthia, I-80126 Napoli, Italy

E-mail: roberto.rosati@polito.it

Abstract. Employing as prototypical systems the metallic single-walled carbon nanotubes (SWNTs), we investigate the electronic propagation in Carbon-based materials, showing that their linear electronic spectra protect the spatial shape of electronic wavepackets from phonon-induced diffusion, up to micrometric scale already at room temperature. To this end, we employ a recently proposed nonlinear Lindblad-based density-matrix approach, which allows us to account for the interplay between phase coherence and dissipation/decoherence, avoiding both huge computational costs of non-Markovian approaches or the limitations of oversimplified dephasing models.

Nowadays, a quite fascinating challenge in nanotechnology is to control the dynamics of electron waves as accurately as in optics.[1] To this purpose, Carbon-based materials such as graphene[2, 3] or metallic single-walled carbon nanotubes (SWNTs)[4] are optimal candidates for dispersionless electronic propagations, thanks to their linear electronic spectra where the Fermi velocity $v_F \sim 10^6\,\mathrm{m/s}$ replaces the speed of light c for photons. In particular, metallic SWNTs can be regarded as the one-dimensional electron waveguides that can in principle provide an electronic alternative to photon-based quantum information processing, as they are synthesized with high accuracy [4, 5, 6]. Although scattering with vacancies or defects can be fairly neglected at first, any implementation in realistic devices requires to determine the impact of electron-phonon processes, which are indicated by experiments as the main source of scattering at intermediate and room temperature [7, 8]. Here, along the lines of recent results [9], we investigate their impact by employing a recently developed density-matrix approach, which enables us to account for both energy dissipation and decoherence effects.[10] We demonstrate that, while in semiconducting SWNTs an electronic wavepacket spreads already for a scattering-free propagation, in metallic SWNTs its shape is essentially unaltered, even in the presence of electron-phonon coupling. Differently from predictions based on the conventional relaxation-time approximation (RTA), our results thus indicate metallic SWNTs as a realistic electron-based platform for information transfer.

In the neighborhood of **K** and **K**' valleys, the free-electron states belonging to the lowest energy subband may be labelled by $\alpha = (k, b, v, \nu)$, where k denotes the continuous wavevector component along the SWNT axis, $b = \pm 1$ and $v = \pm 1$ stands respectively for conduction/valence band and for **K**/**K**' valley, while ν may take the value $\nu = 0, \pm 1$, depending on the geometry of

the SWNT. The corresponding spectrum, which is given by

$$\epsilon_\alpha = b\,\hbar v_F \sqrt{k^2 + (\nu/3R)^2}\ , \tag{1}$$

is gapped (semiconducting nanotube) and, near $k = 0$, parabolic-like (similarly to conventional semiconductors) for $\nu \neq 0$, while for $\nu = 0$ it is gapless (metallic case), with the typical massless Dirac-cone structure.[11] The SWNT phonon spectrum near the **K** and **K′** points includes[11, 12] longitudinal and transverse acoustic modes with sound velocities of about $1.9 \cdot 10^4$m/s and $1.5 \cdot 10^4$m/s respectively, the breathing modes orthogonal to the nanotube surface, with a roughly q-independent spectrum $\hbar\omega_{Br} \simeq 0.14\,\mathrm{eV\AA}/R$, and a couple of optical modes whose energies are about 0.2 eV.

In order to account for energy dissipation and decoherence induced by the nanotube phonon bath on the otherwise phase-preserving electron dynamics, we have applied to the carbon nanotube the formalism introduced in [10] via a numerical solution of the Lindblad-based non-linear density-matrix equation (LBE)

$$\begin{aligned}\frac{d\rho_{\alpha_1\alpha_2}}{dt} = & \frac{\epsilon_{\alpha_1} - \epsilon_{\alpha_2}}{\imath\hbar}\rho_{\alpha_1\alpha_2} + \\ & + \frac{1}{2}\sum_{\alpha'\alpha'_1\alpha'_2,s}\left[\left(\delta_{\alpha_1\alpha'} - \rho_{\alpha_1\alpha'}\right)\mathcal{P}^s_{\alpha'\alpha_2,\alpha'_1\alpha'_2}\rho_{\alpha'_1\alpha'_2} - \left(\delta_{\alpha'\alpha'_1} - \rho_{\alpha'\alpha'_1}\right)\mathcal{P}^{s*}_{\alpha'\alpha'_1,\alpha_1\alpha'_2}\rho_{\alpha'_2\alpha_2}\right] + \text{H.c.}\end{aligned} \tag{2}$$

Here, the first term describes the scattering-free propagation, whereas the second term is a non-linear scattering superoperator expressed via generalized scattering rates $\mathcal{P}^s_{\alpha_1\alpha_2,\alpha'_1\alpha'_2}$, whose explicit form is microscopically derived from the electron-phonon Hamiltonians, with s labelling the various phonon modes. The fully quantum-mechanical density-matrix equation (2) enables us to go beyond the conventional Boltzmann transport equation, which is recovered in the diagonal limit ($\rho_{\alpha_1\alpha_2} = f_{\alpha_1}\delta_{\alpha_1\alpha_2}$),[13] where the generalized scattering rates reduce to the semiclassical rates provided by the standard Fermi's golden rule, $P^s_{\alpha\alpha'} = \mathcal{P}^s_{\alpha\alpha,\alpha'\alpha'}$.

In order to show that carbon nanotubes can be utilised as quantum-mechanical channels for the non-dispersive transmission of electronic wavepackets, we have performed simulated experiments where the shape of an initially prepared wave packet is monitored while it evolves under the effect of the phonon bath. Any initial state can always be written as $\rho = \rho^\circ + \delta\rho$, where ρ° is the homogeneous equilibrium state and $\delta\rho$ describes a localised excitation, whose spatial shape (e.g. Gaussian) can in principle be generated experimentally via a properly tailored optical excitation. The description of the specific optical generation is beyond the aim of the present paper. However, the localisation of the initial wave packet is the crucial aspect in our analysis. A simple choice that captures this essential physical ingredient is an initial state described by an intra-valley conduction-band density matrix $\rho_{\alpha_1\alpha_2} = \delta_{v_1,v_2}\delta_{b_1,1}\delta_{b_2,1}\rho_{k_1\,k_2}$, where

$$\rho_{k_1k_2} = \sqrt{f^\circ_{k_1} f^\circ_{k_2}}\, e^{-\ell|k_1 - k_2|}\ . \tag{3}$$

Here f°_k is the Fermi-Dirac distribution of the conduction-band states k, and the parameter ℓ plays the role of a delocalization length. Indeed for $\ell \to \infty$ the spatially homogeneous equilibrium state $\rho^\circ_{k_1k_2} = f^\circ_{k_1}\delta_{k_1k_2}$ is recovered, whereas for finite ℓ the excitation $\delta\rho$ consists of interstate phase coherence (intraband polarization) determined by the parameter ℓ and whose presence is necessary for producing localized distributions. In particular, in the limit $\ell \to 0$ one obtains the maximally localized wavepacket. Moreover, a distinguished feature of the initial condition in (3) is the absence of nonequilibrium diagonal contributions ($\rho_{kk} = f^\circ_k$), which implies that energy dissipation and decoherence will affect the non-diagonal contributions only; this is the typical situation produced by a weak interband optical excitation.

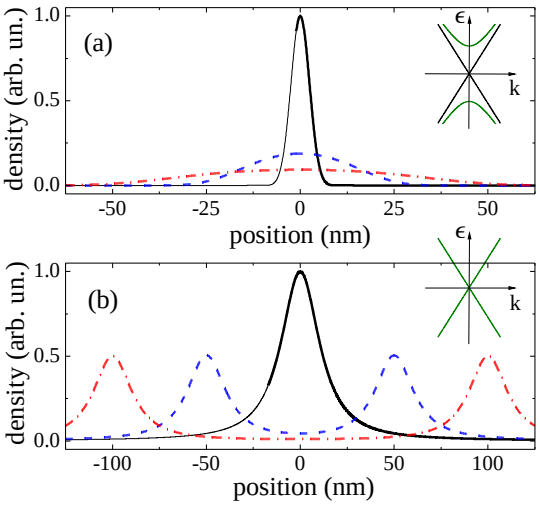

Figure 1. Room-temperature scattering-free evolution in a semiconducting (10,0) SWNT ($\nu = 1$) (a) and in a metallic (12,0) ($\nu = 0$) SWNT (b): Charge density of the maximally-localized ($\ell \to 0$) electronic wavepacket in Eq. (3) as a function of the position along the SWNT axis at three different times: $t = 0$ fs (solid), $t = 50$ fs (dashed) and $t = 100$ fs (dashed-dotted).

We start our discussion by analysing the scattering-free propagation of the initial state (3), i.e. switching off the electron-phonon interaction in Eq. (2). Figure 1 shows the spatial carrier density $n(r_\parallel)$ at different times for the initial state (3), taken at room temperature and in the maximally-localized limit ($\ell \to 0$). The cases of semiconducting and metallic nanotubes are shown in panels (a) and (b), respectively. For the semiconducting nanotube ($\nu \neq 0$) the dispersion relation (see Eq. (1)) at small k reduces to the parabolic spectrum of conventional semiconductor materials and gives rise to the typical classical-like diffusion process, preventing any information transfer via electronic wavepackets. In contrast, for the case of the metallic nanotube ($\nu = 0$), characterised by a linear dispersion, the initial charge peak splits into two identical and shape-preserving components which travel in opposite directions with velocity $\pm v_F$ (see Fig 1(b)), i.e., $n(r_\parallel, t) = n^+(r_\parallel - v_F t) + n^-(r_\parallel + v_F t)$. This non-dispersive propagation is the interesting starting point of our analysis.

We now focus on the metallic nanotube and switch on the electron-phonon coupling to address the crucial question of whether and how energy dissipation and decoherence modify such ideal dispersion-free scenario. To this end, we have performed a set of simulated experiments based on the LBE (2) including all the above introduced phonons. In order to expand the space scale with respect to the ideal scenario displayed in Fig. 1(b), here the delocalization length ℓ in the initial condition (3) is chosen such to get a FWHM value of the initial peak of 0.4μm.

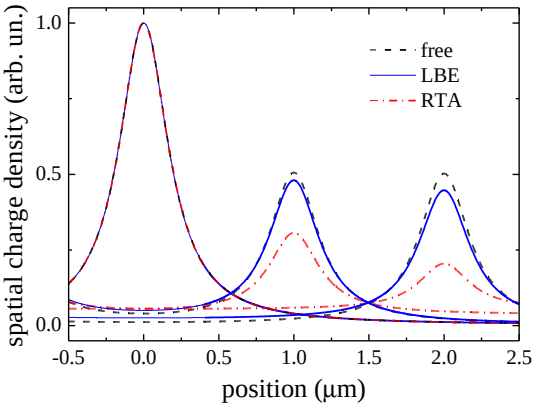

Figure 2. Room-temperature evolution of the electronic wavepacket (3), with ℓ such to provide an initial FWHM of 0.4 μm, in a metallic (12,0) SWNT as a function of the position $r_\parallel$ along the SWNT axis, at three different times: $t = 0$ ps (left peaks), $t = 1$ ps (central peaks) and $t = 2$ ps (right peaks). The solid lines show the effects of the carrier-phonon coupling, accounted for by the LBE (2), compared to the scattering-free (dashed lines) as well as RTA propagations (dot-dashed lines).

Figure 2(a) shows the wavepacket propagation in a (12,0) SWNT at room temperature. The electron-phonon coupling, accounted for by our LBE simulation (solid curve), does not significantly alter the shape with respect to the ideal scattering-free result (dashed curve), so that the transmission is essentially dispersionless up to the micrometric scale (the diffusion time would still increase at lower temperatures, e.g. at 77 K one has a signal attenuation of less than 1% after 1μm). Such a strong suppression of the phonon-induced diffusion predicted by our LBE is mainly due to the negligible effect produced by forward processes (i.e., those which preserve velocities), which do not lead to the scattering non-locality and quantum diffusion speed-up phenomena that occur in semiconducting materials [13]. Remarkably, such uneffectiveness of forward scattering processes occurs despite their electron-phonon couplings are a priori one order of magnitude bigger than the backward ones [11] for acoustic as well as breathing phonons (here the optical modes have a negligible impact due to their high energy[7]). In sharp contrast, the oversimplified RTA strongly overestimates the phonon-induced dissipation, due to its inability to distinguish between forward and backward processes, as shown by the dash-dotted line of Fig.2. Notice that, while semiclassical approaches show a somehow similar forward-scattering suppression, here the off-diagonal nature of the density matrix makes such phenomena highly nontrivial and strictly related to the genuine quantum phenomenon of scattering-induced nonlocality.

In conclusion, differently from what happens in semiconducting materials[10], in metallic SWNTs the impact of the phonon-induced diffusion on the wavepacket propagation is very limited. The scattering-free propagation is thus not just an ideal scenario, and the initial wavepacket propagates at the Fermi velocity with an almost unaltered shape, despite dissipation and decoherence processes are in principle present. Our results indicate that metallic SWNTs are a promising platform to realise quantum channels for the non-dispersive transmission of electronic wavepackets. We thus expect these results will pave the way for advanced optoelectronics with metallic SWNTs.

Acknowledgments

We gratefully acknowledge funding by the Graphene@PoliTo laboratory of the Politecnico di Torino, operating within the European FET-ICT Graphene Flagship project (www.graphene-flagship.eu). F.D. also acknowledges support from Italian FIRB 2012 project HybridNanoDev (Grant No.RBFR1236VV).

References

[1] Kok P, Munro W J, Nemoto K, Ralph T C, Dowling J P and Milburn G J 2007 *Rev. Mod. Phys.* **79**(1) 135–174
[2] Neto A C, Guinea F, Peres N, Novoselov K S and Geim A K 2009 *Rev. Mod. Phys.* **81** 109
[3] Basov D N, Fogler M M, Lanzara A, Wang F and Zhang Y 2014 *Rev. Mod. Phys.* **86**(3) 959–994
[4] Charlier J C, Blase X and Roche S 2007 *Rev. Mod. Phys.* **79**(2) 677–732
[5] Maruyama S, Kojima R, Miyauchi Y, Chiashi S and Kohno M 2002 *Chem. Phys. Lett* **360** 229–234
[6] Arnold M S, Green A A, Hulvat J F, Stupp S I and Hersam M C 2006 *Nat. Nanotechnol.* **1** 60–65
[7] Yao Z, Kane C L and Dekker C 2000 *Phys. Rev. Lett.* **84** 2941
[8] Park J Y, Rosenblatt S, Yaish Y, Sazonova V, Üstünel H, Braig S, Arias T, Brouwer P W and McEuen P L 2004 *Nano Lett.* **4** 517–520
[9] Rosati R, Dolcini F and Rossi F 2015 *Appl. Phys. Lett.* **106** 243101
[10] Rosati R, Iotti R C, Dolcini F and Rossi F 2014 *Phys. Rev. B* **90**(12) 125140
[11] Ando T 2005 *J. Phys. Soc. Jpn.* **74** 777–817
[12] Suzuura H and Ando T 2002 *Phys. Rev. B* **65** 235412
[13] Rosati R and Rossi F 2014 *Phys. Rev. B* **89** 205415